Efficient Detection and Correction of Residual Motion Errors in Airborne SAR Interferometry

P. Prats[1,3], A. Reigber[2], J. J. Mallorqui[1], A. Broquetas[1]
[1]Dept. Signal Theory and Communications, Universitat Politècnica de Catalunya, Barcelona, Spain
{prats,mallorqui,broquetas}@tsc.upc.es
[2]Dept. Computer Vision and Remote Sensing, Technical University Berlin, Berlin, Germany
anderl@cs.tu-berlin.de
[3]Dept. Telecommunications and Engineering Systems, Universitat Autònoma de Barcleona, Barcelona, Spain

***Abstract*—This paper discusses the detection and correction of residual motion errors in airborne SAR interferograms. They usually appear due to the lack of precision in the navigation system. Two techniques existing in the literature to detect such errors are presented, highlighting differences and similarities. The effects of residual motion errors in the final interferogram are mainly two: azimuth phase undulations and azimuth registration errors. A new correction approach is proposed, which corrects both effects in one step, avoiding the use of interpolations. Additionally, the spectral diversity technique, used to estimate registration errors, is critically analyzed. Airborne L-band repeat-pass interferometric data of the German Aerospace Center (DLR) experimental airborne SAR (E-SAR) is used to validate the method.**

Synthetic aperture radar (SAR); interferometry; repeat-pass interferometry; calibration; motion compensation; image registration

I. INTRODUCTION

Airborne synthetic aperture radar (SAR) systems usually record the platform movement to later carry out motion compensation during data processing. Due to the lack of accuracy in the navigation system, residual motion errors appear in the image. The effects of these errors in the final interferogram are mainly two: registration errors and phase undulations, both along the azimuth dimension (note that the variation along range is negligible in a beam-center geometry). Residual motion error effects are mostly noticeable in repeat-pass systems, but the solutions to be presented for their detection and correction can also be applied to single-pass ones.

Regarding the detection of residual motion errors in interferometry, mainly two techniques are described in literature, [1] and [2]. In this paper, both techniques are presented and compared. Additionally, the spectral diversity technique (i.e., splitting of the spectra into subapertures) is analyzed, highlighting the potentials and limitations of using it to measure registration errors [3] as well as residual motion errors. It is important to state that these techniques estimate the differential error between both acquisitions, and not the individual error of each image.

This work was supported by the Spanish MCYT and FEDER funds under project TIC 2002-04451-C02-01.

The second issue of this paper is the optimal correction of residual motion errors [4]. In Section 2.3 a novel correction technique is presented, which removes both registration errors and residual phase errors without the use of interpolations, but by refocusing with a modified motion compensation function.

II. RESIDUAL MOTION ERRORS

The consequences of unmeasured motion of the platform in a SAR image are well stated in the literature: a constant error induces a phase offset, a linear error induces a shift of the impulse response, and a quadratic one induces defocusing, as well as a phase offset [5]. Therefore, mean phase errors along the synthetic aperture will give interferometric phase offsets (phase undulations), and linear components will result in the displacement of the impulse response, leading to registration errors in the final interferogram when residual motion errors are not correlated in both images. It has to be noted that other error sources are not being considered, mainly errors due to the assumption of a reference height during motion compensation. Effectively, the phase error induced in targets at a different height than the reference one can induce the same effects as residual motion errors. Such errors can be minimized with the use of an external DEM, or masking such invalid pixels. From now on, it is assumed that the influence of these errors is negligible. Furthermore, the assumption that master and slave images have been processed in order to have the same azimuth pixel spacing yields the following statement: in airborne SAR interferometry there are azimuth registration errors and azimuth phase undulations because of residual motion errors.

A. Estimation of Residual Motion Errors Measuring the Registration Error

In [1], a technique able to detect residual motion errors was presented. It was based on the measurement of the registration error, as this is one of its two main effects

$$\tilde{\phi}_{err}(x,r) = \int_0^x \frac{4\pi \cdot \Delta t(x',r) \cdot v}{\lambda \cdot r} dx' + C \,, \qquad (1)$$

where λ is the wavelength, Δt is the registration error along azimuth in seconds, v is the forward velocity of the platform, r is the slant range distance and C is an integration constant. The interferogram, or one of the images, can be phase corrected using this information.

B. Direct Estimation of Residual Motion Errors with Spectral Diversity

The second approach described in the literature [2], uses the spectral diversity technique (i.e. splitting of the spectra, and in this case, the azimuth spectra), either by using two interferograms processed with different squints, or by splitting the spectra of both images to generate two low resolution interferograms. The obtained differential phase is indeed the *derivative of the residual motion errors*. Effectively, both low resolution interferograms have been focused with different parts of the track, so that the resulting phase error might be different if the error varies during the data acquisition:

$$\begin{aligned} \phi_A(x,r) &= \phi_{topo}(x,r) + \phi_{errA}(x,r) \\ \phi_B(x,r) &= \phi_{topo}(x,r) + \phi_{errB}(x,r), \end{aligned} \tag{2}$$

where ϕ_{errA} and ϕ_{errB} are the resulting phase errors along interferograms A and B, respectively. When obtaining the differential interferogram, the topographic information is cancelled, leaving only the phase error difference between two parts of the track, i.e., the derivative of residual motion errors:

$$\phi_{diff}(x,r) = \phi_A(x,r) - \phi_B(x,r) = \phi_{errA}(x,r) - \phi_{errB}(x,r). \tag{3}$$

Therefore, the differential phase must be integrated to obtain the estimated residual motion error [2]

$$\tilde{\phi}_{err}(x,r) = \int_0^x \frac{\phi_{diff}(x',r)}{\Delta x(r)} dx' + C, \tag{4}$$

where Δx is azimuth distance between the center of both subapertures

$$\Delta x(r) = \left(\tan(\beta_1) - \tan(\beta_2)\right) \cdot r, \tag{5}$$

where β_1 and β_2 are the squint centers of each subaperture. This distance is a key parameter, as it has to be small enough to be able to track fast variations of residual motion errors. The bandwidth of the subapertures is the second important parameter. The undulations visible in the interferogram are the result of the averaging of the true residual motion error along the synthetic aperture: a long aperture cancels out frequency components much higher than its own bandwidth. Consequently, the larger the subaperture, the less accurate the estimation of the residual motion error gets at a given along-track position. This fact also becomes important when applying the correction. If a small bandwidth is used for the subapertures, then fast variations of residual motion errors are detected. However, phase undulations present in the interferogram might not be so fast due to the aforementioned averaging. Therefore, the correction of phase undulations by directly multiplying the phase correction to the interferogram, as suggested in [2], might lead to overcompensation. The solution presented in section 2.3 circumvents this problem. Note also that the estimation is made on a pixel by pixel basis, as stated in equations (2)-(4). However, the differential phase is very noisy [2] [3], so a spatial averaging is strongly recommended, taking into account that the differential phase is almost constant along range in a beam-center geometry. In a similar way, taking into account that

$$\tilde{\phi}_{err} = -\frac{4\pi}{\lambda} \Delta r, \tag{6}$$

where Δr is the residual motion error in line of sight, Δy and Δz displacements from the ideal trajectory can be obtained using two estimated profiles Δr_1 and Δr_2 of residual motion errors at two different ranges.

C. Residual Motion Compensation

Up to now, in order to correct the effects of residual motion errors, a phase correction was usually multiplied to one of the images, followed by a resampling in order to correct misregistration. However, a better approach is possible [4]. As both effects of residual motion errors (misregistration and azimuth phase undulations) have the same origin, they can also be corrected in one step. Once the differential motion error is known, one can also correct for the phase errors by modifying accordingly the matched filter function used for azimuthal SAR focusing. Therefore, a time consuming and imprecise interpolation of the data is not necessary. Such a residual motion compensation step requires decompression of the data along the azimuth dimension (as the assumption that the data are already focused is made, so there is no need to reprocess them again), complex multiplication of the data with $-\phi_{err}$ in time domain, and subsequently again a compression of the data. Decompression must be carried out for each range, so that the length of the impulse response after azimuth decompression precisely corresponds to the one of the raw data. A second approach would be to include the estimated residual motion error in the navigation data and reprocess from the raw data again. However, as the estimated errors are normally small (less than 15 cm), the proposed approach should be selected if processing time is a key issue.

The decompression-phase correction-compression approach is more accurate than interpolation and has the computational burden of 4 additional FFT's along azimuth. It was found that when using modern FFT's implementations, the proposed approach can even be faster than the interpolation / phase multiplication approach. The correction can be applied either on one image, or alternatively fractions of it on both images. In both cases some errors are corrected, but at the same time others induced. However, it has to be noted that the induced motion errors are of the same magnitude as the existing ones. The key point is that differential errors are corrected, i.e. residual motion errors *are the same in both images*.

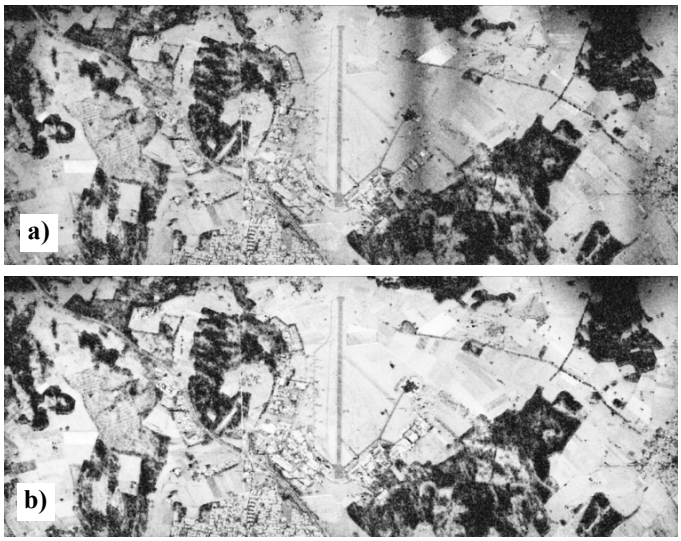

Figure 1. Coherence before (a) and after (b) applying the proposed correction method.

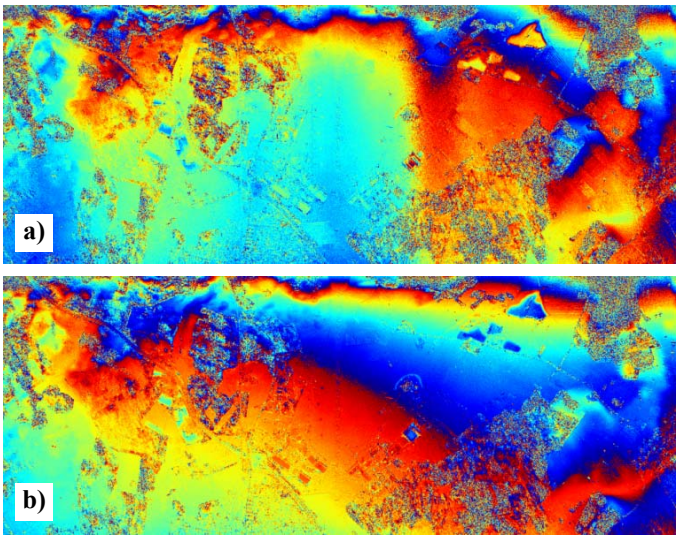

Figure 2. Flattened phase before (a) and after (b) applying the proposed correction method.

Consequently, the interferogram will appear with no registration errors nor azimuth phase undulations. The most accurate approach is to apply 50% of the correction to each image as it is unknown how much error corresponds to each of them.

It is assumed that errors result mainly from vertical and horizontal displacements and not from errors in the measurement of the forward velocity. This approximation is quite accurate, as for the same effect on the misregistration, a much stronger velocity error is necessary.

D. *Discussion on the Estimation of Registration Errors with Spectral Diversity*

The suggested technique in [1] to measure the registration error was [3], based on spectral diversity. The solution for the estimated registration error is:

$$\Delta t = \frac{\phi_{diff}}{2\pi \cdot (fc_1 - fc_2)}, \tag{7}$$

where fc_1 and fc_2 are the center frequencies of each subaperture. To obtain this result, [3] assumes that Δt is the same for both subapertures, a fact that might not be true in the presence of residual motion errors. As already commented, the displacement of the impulse response is related to the linear component of the motion error along the synthetic aperture. Only as long as the error is exactly linear along the synthetic aperture, the spectral diversity technique results in a correct estimation of the registration error. Of course, several parameters must be taken into account, most importantly the processing bandwidth, which specifies the length of the synthetic aperture, and the accuracy of the navigation system. In any case, the most precise estimation of the registration error can be obtained using the maximum separation between subapertures, as the linear trend that induces registration errors is better estimated.

E. *Practical Considerations*

Some differences can be pointed out between the techniques presented in sections II.A and II.B. The former computes the correction from the registration error, while the latter uses the differential phase between subapertures. This implies that, given a good estimation of the registration error is used, II.A estimates the phase undulations appearing in the interferogram, and not the *true* residual motion error. That is to say, it estimates a smoothed version of residual motion errors. Only when the error is linear along the synthetic aperture, II.A and II.B result in the same estimated residual motion error. Therefore, the second technique is better suited to detect fast variations (with the appropriate subaperture configuration) than the first technique, thus obtaining a better estimation of residual motion errors. When applying the correction technique presented in II.C, the usage of II.B will result in a better performance of the overall correction process.

From the application point of view, both methods are equally valid in the sense of getting rid of phase undulations. However, in case of II.A, the obtained interferogram might still not have the maximum possible coherence. The true residual motion error is not corrected here, and phase artifacts due to higher order terms, *which are not common to both images*, do not cancel during interferogram generation.

It is important to note that, when II.A uses [3], it is very closely related to II.B. Effectively, using (7), (1) can be expressed as:

$$\tilde{\phi}_{err}(x,r) = \int_0^x \frac{\phi_{diff}(x',r)}{(\sin(\beta_1) - \sin(\beta_2)) \cdot r} dx' + C, \tag{8}$$

Note that this result is exactly the same as (4), but having sinus instead of tangents, which are similar for small values of β. However, due to the different interpretations given to

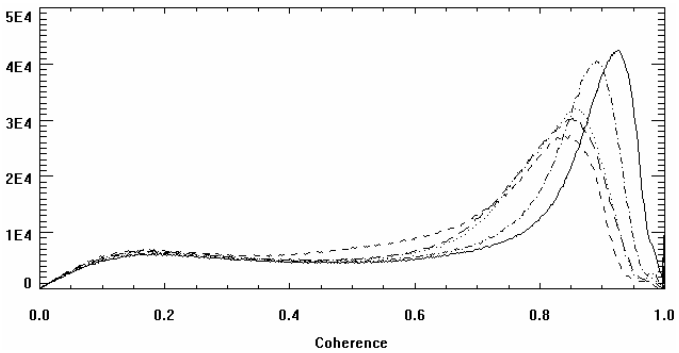

Figure 3. Coherence histograms with different subaperture configurations. Original Coherence (dashed), center ±7.5 Hz and bandwidth 30 Hz (solid), center ±30 Hz and bandwidth 60 Hz (dash-dot), center ±50 Hz and bandwidth 100 Hz (dotted), interpolated using [3] (long dashes).

spectral diversity differential phase, results might not be exactly the same, as already pointed out.

III. Experimental Results

To validate the proposed method, with any loss of generality, airborne repeat-pass E-SAR data was used. Measurements were made at L-band (1.3 GHz) with a bandwidth of 100 MHz and a pulse repetition frequency *PRF* of 400 Hz over the test site of Oberpfaffenhofen, Germany. The flight altitude is 3200 m, and the velocity of the platform is 91 m/s. The data have been processed with a bandwidth half of the full *PRF*, leading to an effective *PRF* of 200 Hz, and a Hamming window (α = 0.54) in both azimuth and range dimensions. Range registration has been carried out using the scaling properties of the Extended Chirp Scaling Algorithm (ECSA) [6].

The original coherence and interferometric flattened phase appear in Fig. 1(a) and Fig. 2(a). The black stripes in the middle of Fig. 1(a) and in some other areas represent coherence losses due to residual motion errors. The Oberpfaffenhofen test site is almost flat, so that observed azimuth phase undulations in Fig. 1(a) are mainly due to residual motion errors.

To estimate the derivative of residual motion errors, spectral diversity has been configured with a separation between subapertures of 15 Hz, centered at ±7.5 Hz, and a bandwidth of 30 Hz (there exists overlap). Using (4), residual motion errors have been estimated and the suggested correction method has been applied to the data (50% to each image). Figures 1 (b) and 2 (b) show the corrected coherence and flattened phase, respectively. The improvement is evident: both registration errors and azimuth phase undulations disappeared almost completely. It must be noted that the obtained phase should be further calibrated, as some flat-earth-phase-like phase components remain in both range and azimuth dimensions, which are related to residual motion errors [7].

Coherence histograms have been computed with different subaperture configurations. Results are shown in Fig. 3. It can be observed that a larger separation between subapertures causes a lower coherence, as residual motion errors are worse estimated. Also, coherence after coregistering using [3] has been computed, using half the bandwidth for each subaperture without overlap. The small improvement in this case is also due to non-common phase artifacts after azimuth focusing, as residual motion errors have not been corrected. Due to the chosen bandwidth for each subaperture, the estimated registration error using [3] is probably quite accurate, as the linear trend of residual motion errors is estimated. Note that this solution and the one using the proposed method with center of subapertures at ±50 Hz and bandwidth of 100 Hz (dotted), are very similar, as in both cases the same configuration for spectral diversity has been used. However, in the former an interpolation has been carried out, while with the latter the new correction approach has been used.

IV. Conclusions

An analysis of residual motion errors has been carried out, pointing out their two main consequences: azimuth phase undulations and azimuth registration errors. This allows correcting both in one step with a residual motion compensation, avoiding in this way the critical interpolation step commonly used to correct registration errors. Results with L-band data have been shown, proving the validity of the method. Direct estimation of residual motion errors using spectral diversity [2] is recommended, as it does not make any assumption, leading to a more accurate result when used in conjunction with the proposed correction. Special care must be taken with the separation and bandwidth of subapertures, as they play an important role to be able to track fast variations. Note also, that the algorithm can be easily made iterative for better detection of fast variations.

V. Acknowledgment

The authors would like to thank the German Aerospace Center (DLR) for supplying the E-SAR data.

VI. Literature

[1] A. Reigber, "Correction of residual motion errors in airborne SAR interferometry," IEE Electron. Lett., vol. 37, no. 17, pp. 1083-1084, Aug. 2001.

[2] P. Prats and J. J. Mallorqui, "Estimation of azimuth phase undulations with multisquint processing in airborne interferometric SAR images," IEEE Trans. Geosci. Remote Sensing, vol. 41, no. 6, pp.1530-1533, June 2003.

[3] R. Scheiber and A. Moreira, "Coregistration of interferometric SAR images using spectral diversity," IEEE Trans. Geosci. Remote Sensing, vol. 38, pp. 2179-2191, Sept. 2000.

[4] P. Prats, A. Reigber, J. J. Mallorqui, "Interpolation-free coregistration and phase-correction of airborne SAR interferograms," *IEEE Trans. Geosci. and Remote Sensing*, in press.

[5] M. Bara, J. Monne, and A. Broquetas, "Navigation systems requirements for airborne interferometric SAR platforms," Proc. IGARSS, 1999, pp. 2158-2160.

[6] A. Moreira, J. Mittermayer, and R. Scheiber, "Extended chirp scaling algorithm for air- and spaceborne SAR data processing in stripmap and scansar imaging modes," IEEE Trans. Gesoci. Remote Sensing, vol. 34, no. 5, pp. 1123-1136, September 1996.

[7] R. Scheiber, "A three-step phase correction approach for airborne repeat-pass interferometric SAR data," *Proc. IGARSS'03*.